Modeling and test-analysis correlation study of a five-storey whare (building) using in-situ measurements

H. Shirzadi, B. Moaveni
Tufts University, Medford MA, USA

Y. Eftekhar Azam
University of New Hampshire, Durham NH, USA

Kaveh Andisheh
HERA, Auckland, New Zealand.

ABSTRACT

This paper presents the dynamic testing and system identification of a five-storey steel moment-resisting frame whare (building) in New Zealand, equipped with passive viscous dampers. The whare (building's) ambient vibrations were recorded over 60 hours using 24 accelerometers distributed across five levels. An optimal sensor placement approach was utilised to minimise the number of sensors and costs while maximising the information gained. Sensor placement was guided by Kammer's methodology (Kammer, 1991), which optimises modal partition linear independence, and is further refined to accommodate site-specific constraints. The stochastic subspace identification (SSI) method was applied to the recorded data to extract the whare (building's) modal parameters, including natural frequencies and mode shapes. This study provides valuable insights into the integration of field testing and numerical modeling for an enhanced understanding of the dynamic behavior of complex structural systems in multi-storey ngā whare (buildings) located in high seismicity areas. Designed to withstand severe ngā rū whenua (earthquakes) with minimal structural damage, the findings contribute to developing robust model updating techniques and advancing rū whenua (earthquake) pūkaha (engineering) by improving seismic performance predictions for complex structures.

1 INTRODUCTION

Vibration-based damage detection methods, particularly those relying on modal parameters, have demonstrated great promise in identifying structural damage in civil infrastructure. Modal parameters, such as natural frequencies and mode shapes, can be accurately determined through ambient or forced vibration testing. For large-scale operational structures, ambient vibration testing is typically favored since forced testing often requires interrupting normal operations. By leveraging these extracted modal parameters, finite element (FE) model updating techniques can efficiently detect, localise, and evaluate damage severity, which is usually reflected in changes to the structure's physical properties (Friswell & Mottershead, 1995). Extensive reviews of vibration-based methods for finite element model updating and damage detection can be found in the works of Ereiz et al. (2022) and Sohn et al. (2003).Researchers have utilised both deterministic (Moaveni et al., 2010; Teughels & De Roeck, 2004) and probabilistic (Behmanesh et al., 2015; Rocchetta et al., 2018; Sohn & Law, 1997) approaches in correlating the dynamic testing findings to the tuning of the existing model of the structure.

The case study whare (building) in this paper, situated in Christchurch, New Zealand, is a five-storey moment-resisting frame equipped with passive viscous dampers. Figure 1 presents an aerial view of the whare (building) and its surroundings. Vehicular traffic on the adjacent streets and passing trains contribute to the excitation of the structure.

Figure 1 Aerial view of the case study whare (building)

2 SENSOR PLACEMENT AND DYNAMIC TESTING

In this study, the Kammer method (Kammer, 1991) was used to determine the optimal sensor placement when only a limited number of sensors could be installed on the structure.. The objective of this method is the optimal sensor placement to identify target mode shapes in structural systems. The approach begins with a candidate set of sensor locations, selected based on the modal kinetic energy distribution, which quantifies the dynamic contribution of each degree of freedom to the target modes. The candidate set is then reduced to an optimal subset by maximising the Fisher information matrix, thereby minimising the covariance matrix of estimation errors. Key steps include computing the kinetic energy distribution, evaluating sensor contributions using the Fisher information matrix, and employing eigenvalue analysis to rank sensor locations. The fractional eigenvalue distribution and effective independence distribution are used to eliminate low-contributing sensors, ensuring optimal placement for accurate modal identification. The optimal sensor placement approach requires an estimate of the structure's mode shapes. In this study, the ETABS model used by the rangahau (research) team is utilised as an approximation of the mode shapes of the real structure. It is assumed that the floors behave as rigid diaphragms, allowing the in-plane displacement distribution on each floor to be represented by three displacement components. Two corners of the structure—the northeast and southwest corners—were selected as initial sensor placement candidates. At the northeast corner, two sensors are assumed to be installed to measure displacements in both the x and y directions, while at the southwest corner, a single sensor is assumed to be placed in the x direction. The degrees of freedom and sensor locations on each floor are illustrated in Figure 2, where the starting points of the vectors indicate the sensor positions.

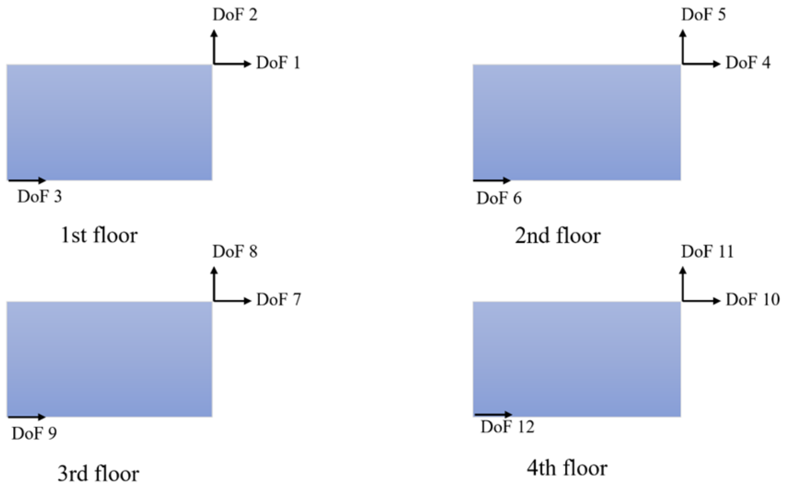

Figure 2 Definition of the degrees of freedoms

The optimal sensor placement scheme depends on the number of structural modes intended for measurement. In this study, the goal was to capture the first five modes of the structure. While it is theoretically possible to identify all modes, ambient vibrations make it challenging to excite higher and more complex modes. The first five modes of the FE model include two lateral modes in the x and y directions, as well as one torsional mode. Given the sensor locations, Kammers' methodology is applied to evaluate the contribution of each sensor in capturing the target modes, as illustrated in Figure 3.

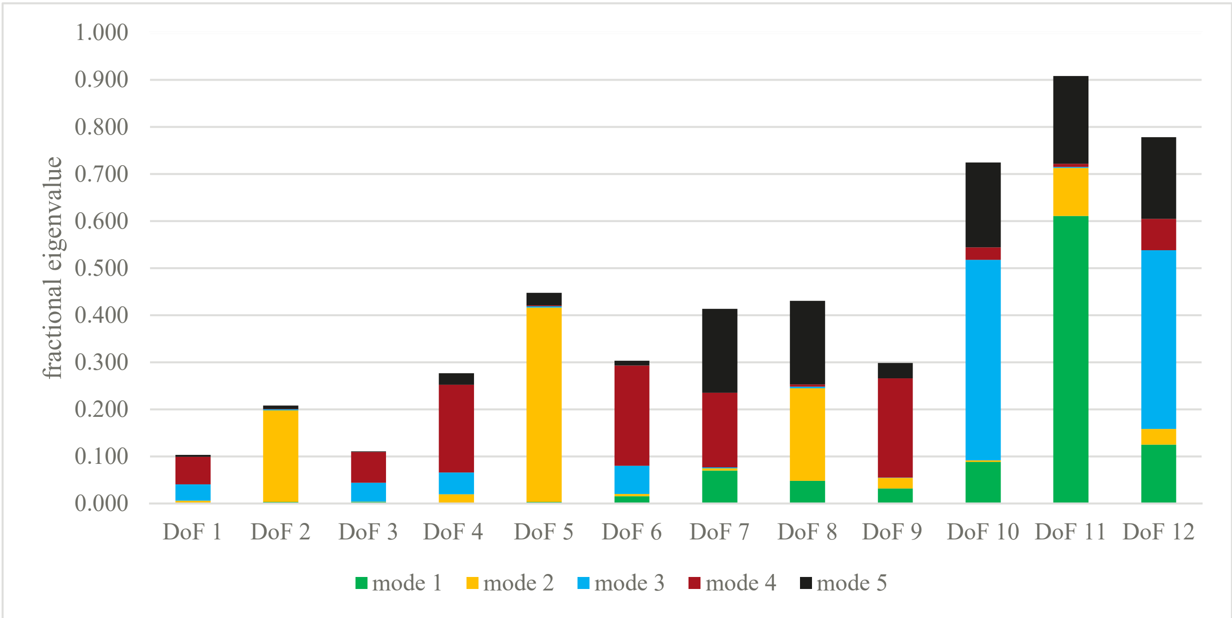

Figure 3 the fractional eigenvalue distribution over all DoFs considering the first 5 modes

Figure 3 presents the contribution of different Degrees of Freedom (DoFs) and the corresponding sensor DoFs—*i.e.,* the directions in which the sensors record acceleration—in capturing the first five structural modes. This highlights the optimal sensor placement strategy. DoFs 11 and 12 are the most critical, as they exhibit the highest contributions across multiple modes, making them prime locations for sensor placement. Additionally, DoFs 10, 5, 6, 7, 8, and 9 also play significant roles in capturing specific modes and should be considered for additional sensors. In contrast, DoFs 1, 2, 3, and 4 have relatively low contributions, suggesting they are less effective for modal identification. To ensure efficient sensor placement, priority should be given to DoFs 11 and 12, while strategically incorporating sensors at DoFs 10, 5, 6, 7, 8, or 9 as needed.

Due to access limitations, placing sensors on the first floor was not possible, leading to slight modifications in the final sensor placement scheme. The revised configuration includes two stations at the ground level, each equipped with three sensors (x, y, z) to capture train-induced vibrations and facilitate the calculation of Horizontal-to-Vertical Spectral Ratio (HVSR) curves (Konno & Ohmachi, 1998), which provide valuable insights into the soil properties beneath the whare (building). No sensors were installed on the first floor. On the second floor, four stations were established, each with two sensors (x, y), while the third and fourth floors each have two stations with the same sensor configuration. Finally, a single station was placed on the fifth floor, also equipped with two sensors (x, y). This arrangement ensures effective data collection while accommodating accessibility constraints. The overall sensor placement on the structure is illustrated in Figure 4, while Figure 5 provides a close-up view of how the sensors are mounted.

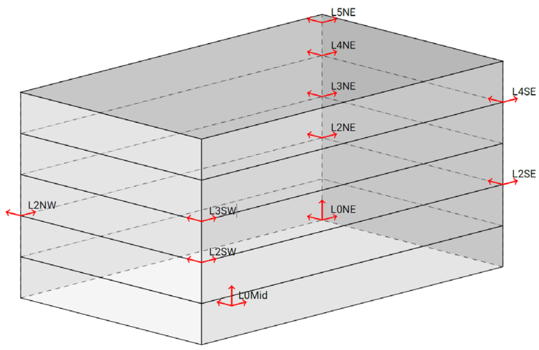

Figure 4 location of the sensors on the structure

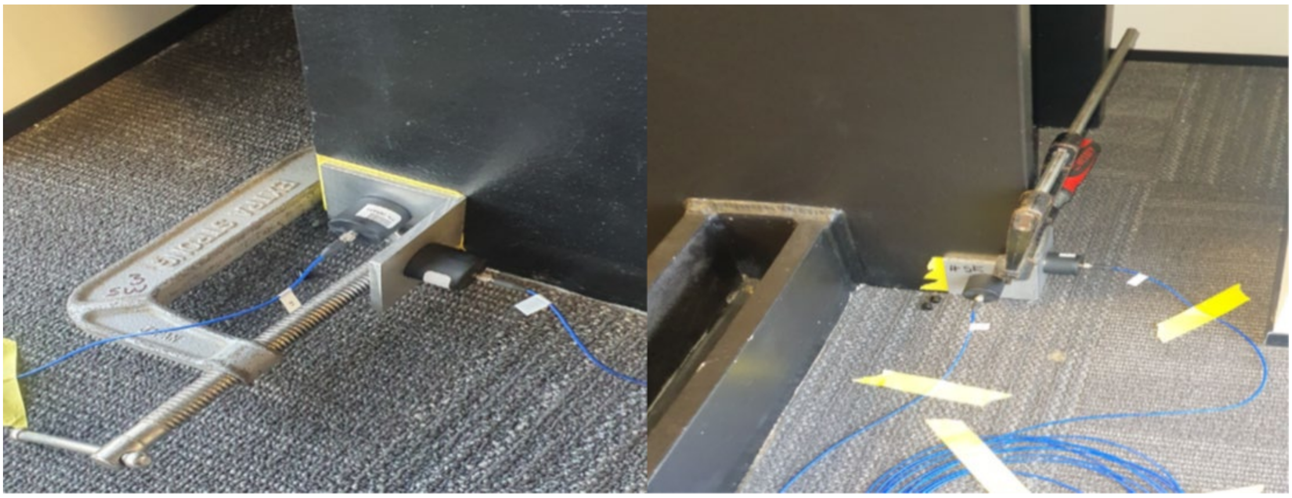

Figure 5 sensors mounted on a steel gusset plate using a right-angle bracket.

The data collection process spanned from June 7th at 18:56 to June 10th at 10:59, with measurements recorded every five minutes, resulting in 734 datasets totaling approximately 100 GB. The data was acquired from 24 sensors at a high sampling rate of 2048 Hz. To enhance data quality, several preprocessing steps were applied, including filtering, down sampling, and spike removal. A bandpass FIR filter of order 8192 was used, with cut-in and cut-off frequencies set at 0.5 Hz and 20 Hz to isolate relevant structural vibrations while removing low-frequency rigid body modes and high-frequency noise. The data was then down sampled from 2048 Hz to 256 Hz to reduce storage size and computational load while preserving critical modal information. Additionally, a spike removal algorithm was implemented to eliminate abnormal signal fluctuations. This method involved iteratively detecting spikes by identifying points exceeding 50 ngā wā (times) the standard deviation of the signal. A window of 200 samples was then applied around each detected spike, and the affected values were replaced through linear interpolation between the window's endpoints. This process ensured that transient anomalies were effectively removed without distorting the overall signal characteristics, resulting in cleaner and more reliable data for subsequent analysis.

For the cleaned data, Root Mean Square (RMS) values of the signals were computed for each five-minute interval and plotted for the two sensors located at the roof level. These plots reveal a daily trend, where excitation levels are lower during nighttime hours when the whare (building) is unoccupied. Additionally, some spikes are observed in the RMS data, likely corresponding to datasets where a train passed by the whare (building), causing a significant increase in structural excitation. The RMS values are presented in Figure 6. Furthermore, the power spectral density (PSD) of the response for these channels was computed for one dataset, as shown in Figure 7. The first three natural frequencies of the structure are clearly visible in the PSD plots, with peaks annotated to indicate the corresponding structural modes.

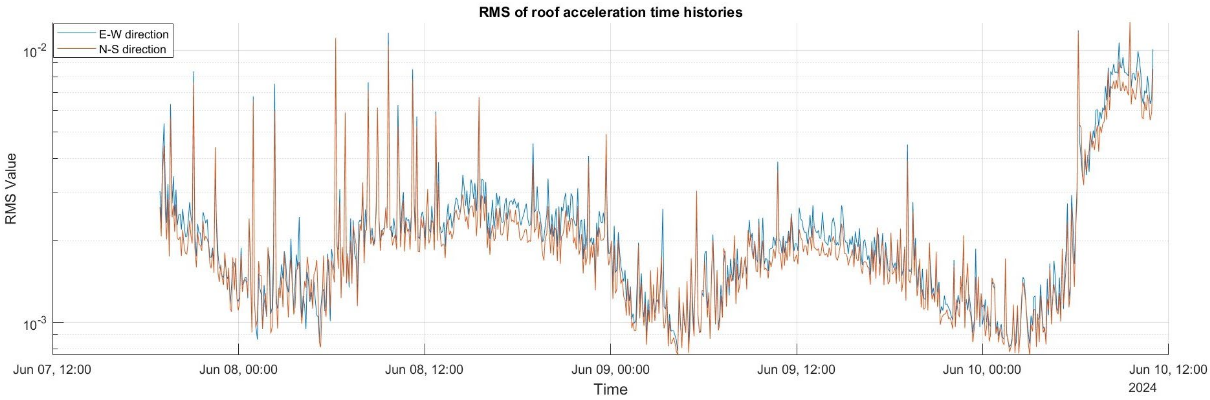

Figure 6 Root mean square of roof acceleration wā (time) histories calculated for each 5 minutes of data

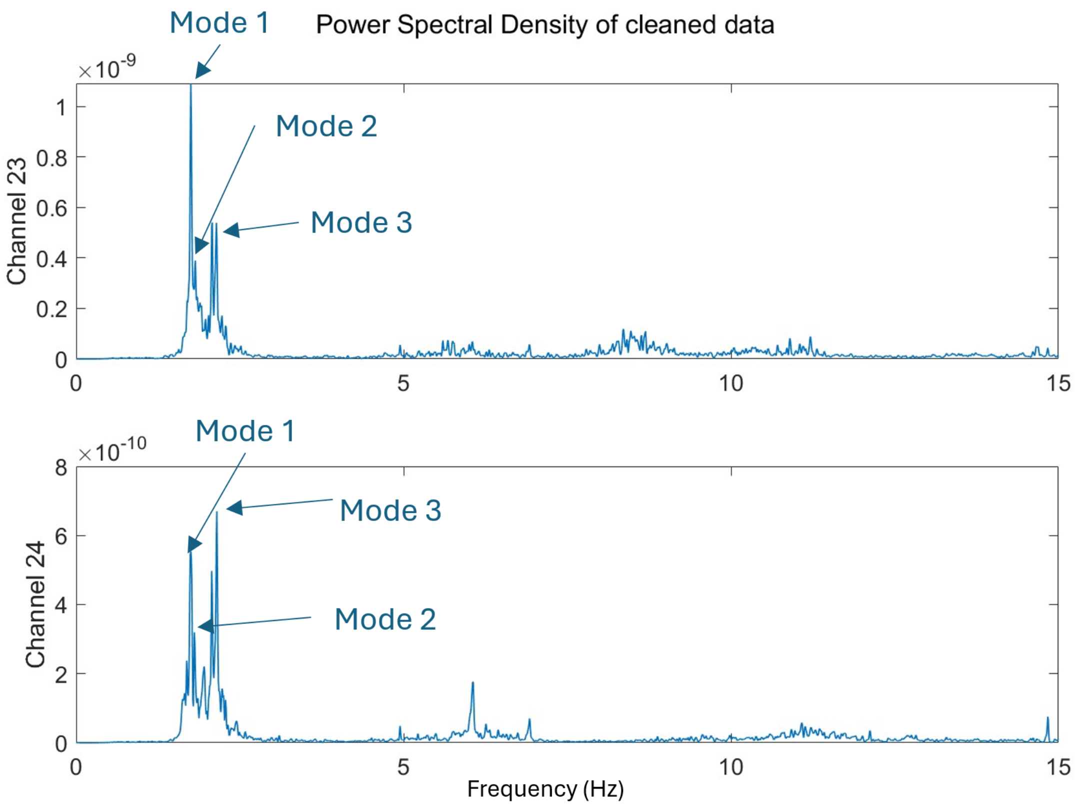

Figure 7 Power spectral density of the two sensors located at the roof level showing peaks in the structure's natural frequencies.

3 SYSTEM IDENTIFICATION

The data-driven stochastic subspace system identification (SSI-DATA) (Peeters, 2000; Van Overschee & De Moor, 2012) method is employed to estimate mode shapes, natural frequencies, and damping ratios. This method fits a linear state space model to output-only measurements under broadband excitation, providing estimates for the state matrix A and output matrix C in the stochastic state-space model:

$$\begin{aligned} x_{k+1} &= Ax_k + w_k \\ y_k &= Cx_k + v_k \end{aligned} \quad (1)$$

Here, x is the system state vector, y is the measurement vector, and w and v represent input and output white noise, respectively. The modal parameters are derived from matrices A and C. In the first step the Hankel matrix H is formed from wā (time) historey acceleration measurements, divided into "past" H_p and "future" H_f partitions:

$$H = \begin{bmatrix} H_p^T & H_f^T \end{bmatrix}^T \quad (2)$$

Then the projection P_α is computed as $P_\alpha = H_f H_p^T \left(H_p H_p^T\right)^+ H_p$. Using singular value decomposition (SVD), P_α is factorised as $P_\alpha = U\Sigma_v V^T$. Afterwards, model reduction is performed by retaining the n largest singular values:

$$P_\alpha \approx U_n \Sigma_n^{1/2},\ \hat{X}_\alpha \approx \Sigma_n^{1/2} V_n^T \quad (3)$$

State-space matrix estimation is performed by creating a shifted Hankel matrix, and the shifted Kalman filter sequence $\hat{X}_{\alpha+1}$ as $\hat{X}_{\alpha+1} = P^{+}_{\alpha-1} P_{\alpha-1}$ .The state-space matrices $\hat{A}$ and $\hat{C}$ are estimated as:

$$\begin{bmatrix} \hat{A} \\ \hat{C} \end{bmatrix} = \begin{bmatrix} \hat{X}_{\alpha+1} \\ Y_{\alpha|\alpha} \end{bmatrix} \hat{X}^{+}_{\alpha} \quad (4)$$

Modal Parameter Extraction is done by performing eigenvalue analysis on $\hat{A}$.

$$\Lambda = \Psi^{-1} \hat{A} \Psi \quad (5)$$

The continuous-time eigenvalue matrix Λ_c is derived as $\Lambda_c = \frac{\ln(\Lambda)}{\Delta t}$ Natural frequencies ω_i and damping ratios ξ_i are computed as:

$$\omega_i = |\lambda_{c,2i-1}|,\ \xi_i = -\frac{\mathrm{Re}\,(\lambda_{c,2i-1})}{\omega_i} \quad (6)$$

And finally, the Mode shapes Φ are obtained as $\Phi = \hat{C}\Psi$. In this study, the numerical implementation developed by Monteiro (2022) is utilised to extract modal parameters from acceleration measurements. Figure 8 presents the stabilisation diagram for the natural frequencies from one of the datasets, demonstrating that the first three structural modes remain stable across a broad range of model orders.

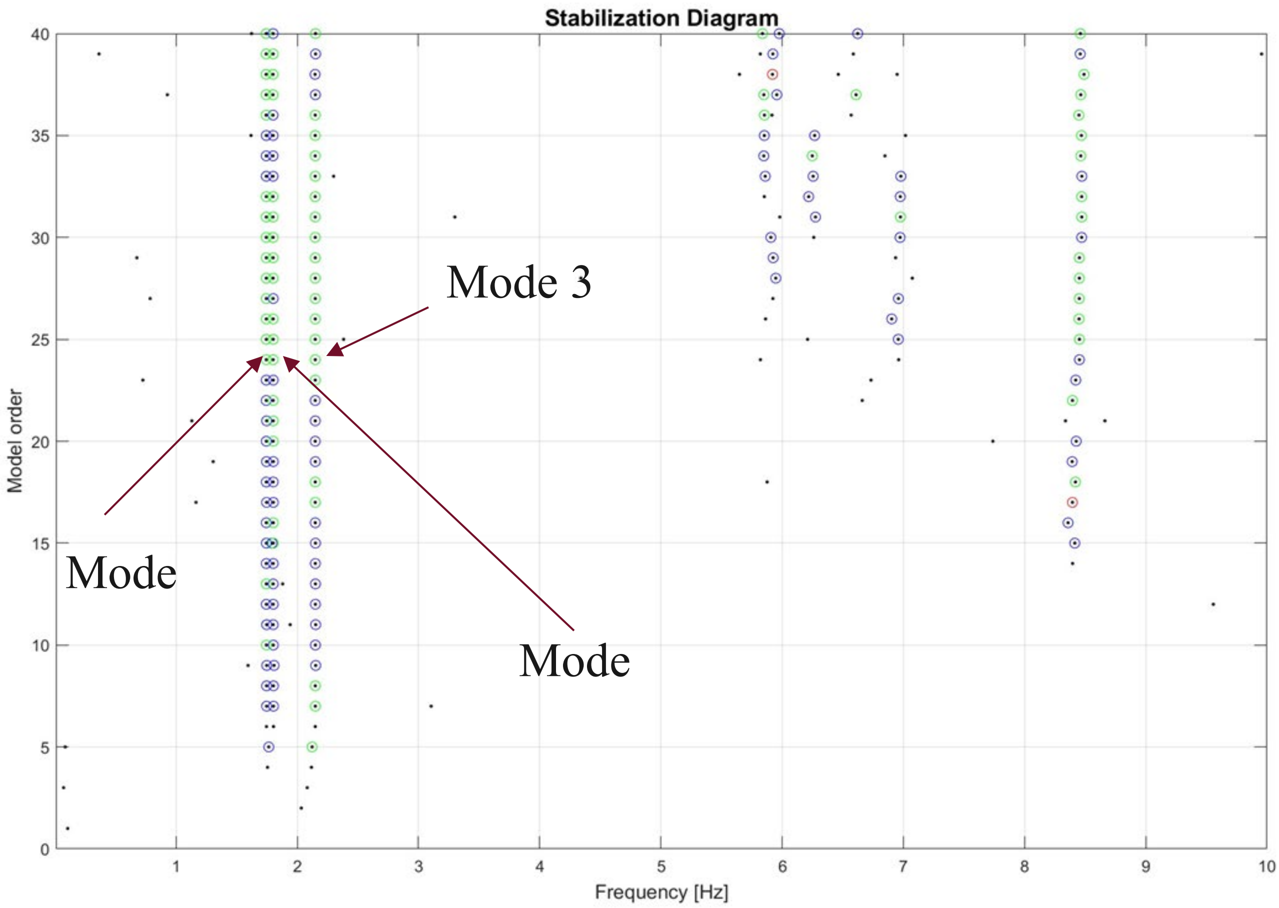

Figure 8 Stabilisation diagram of the natural frequencies

The natural frequencies and damping ratios for the third measured dataset have been identified for the first three modes of the structure. Mode 1, which corresponds to the first mode in the N-S direction, has a natural frequency of 1.76 Hz with a damping ratio of 1.8%, and its mode shape is almost entirely aligned in the N-S direction. Mode 2, representing the first mode in the E-W direction, has a natural frequency of 1.78 Hz and a damping ratio of 2.3%. However, unlike the N-S mode, this mode exhibits a small component in the perpendicular direction, which could be attributed to the offset between the center of mass and the center of stiffness of the whare (building). Mode 3, the first torsional mode, exhibits a natural frequency of 2.14 Hz with a damping ratio of 2.1%. The identified mode shapes for these modes have been extracted and are illustrated in Figure 9, providing a clear visualisation of the structural response at these frequencies.

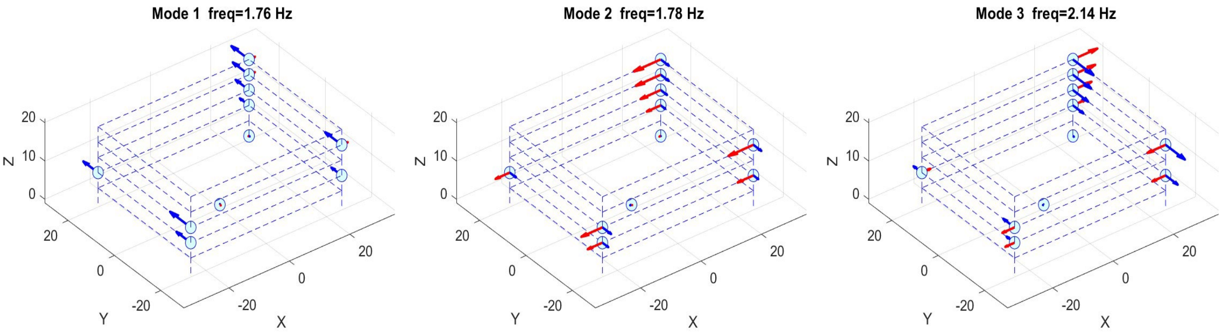

Figure 9 Identified mode shapes of the third dataset. left) the first mode is the N-S direction middle) the first mode in the E-W direction right) the first torsional mode.

The system identification process was performed for all datasets, and the results for the first three natural frequencies and damping ratios are presented in Figure 10. The identified natural frequencies exhibit some variability across the datasets, which could be influenced by environmental factors, such as temperature fluctuations between day and night, as well as variations in the level of excitation. However, despite these influences, the variation in natural frequencies remains relatively small compared to the significant fluctuations observed in the damping ratios. This suggests that while frequency estimates are generally stable, damping ratios are more sensitive to external conditions and measurement uncertainties.

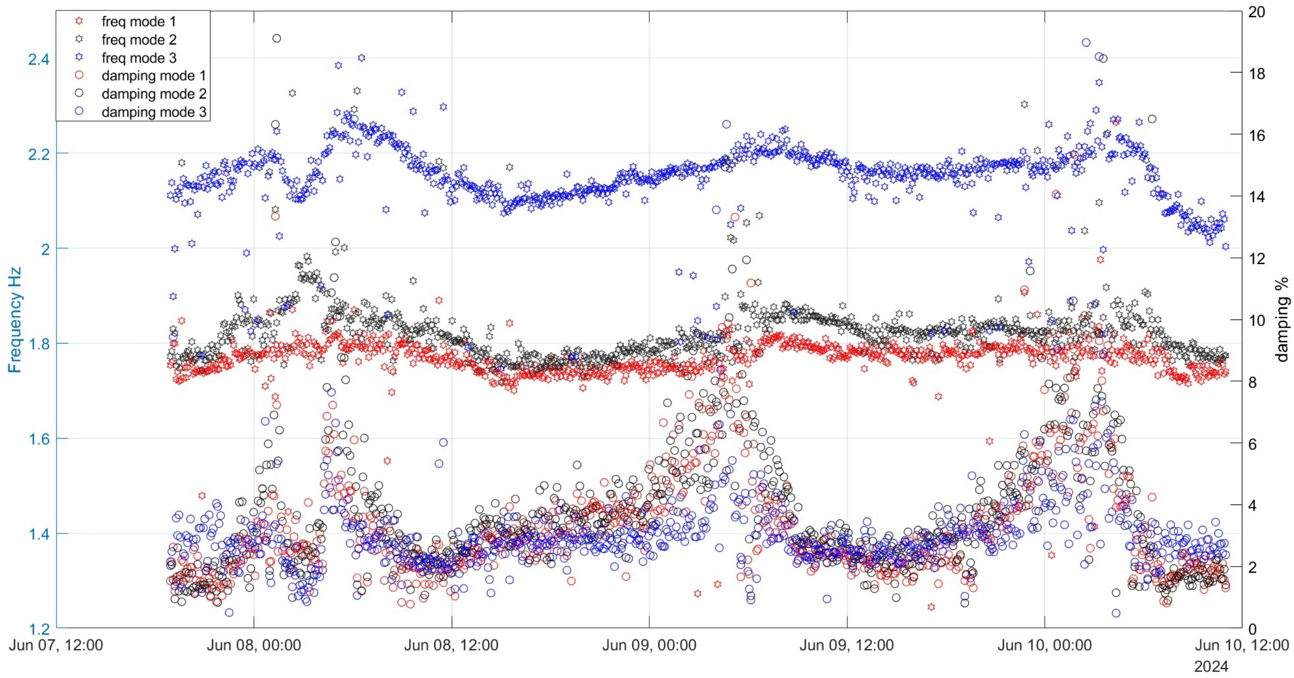

Figure 10 The first three natural frequencies and damping ratios calculated for all of the measured datasets.

4 CONCLUSION

This study presents a comprehensive test-analysis correlation of a five-storey steel moment-resisting frame whare (building) equipped with passive viscous dampers in New Zealand. Through ambient vibration testing, modal parameters were extracted using stochastic subspace system identification (SSI-DATA), providing key insights into the whare (building's) dynamic behaviour. An optimal sensor placement strategy was implemented based on Kammer's methodology, ensuring efficient data acquisition while accommodating site-specific constraints. The system identification process, conducted over 60 hours of monitoring with 24 sensors, successfully extracted the first three natural frequencies, damping ratios, and mode shapes. The results indicate that natural frequencies remain relatively stable, with minor variations potentially attributed to environmental factors such as temperature changes and excitation levels. In contrast, damping ratios exhibit greater variability, suggesting a higher sensitivity to external influences. Additionally, the mode shapes of the structure align with expected patterns, with minor deviations in the E-W mode, likely due to the offset between the center of mass and the center of stiffness. The findings contribute to the advancement of model updating techniques and improve seismic performance predictions for complex structures. This study underscores the importance of integrating field measurements with numerical modeling, providing a robust foundation for future structural taha tinana (health) monitoring and rū whenua (earthquake) Pūkaha (engineering) applications.

ACKNOWLEDGMENT: This article's rangahau is part of a larger research project led by HERA and supported by the Endeavour Fund administered by Te Hīkina Whakatutuki - The Ministry of Business, Innovation and Employment (MBIE) titled "Developing a Construction 4.0 transformation of Aotearoa New Zealand's construction sector. Māori references use the Waikato-Tainui meta (dialect) to acknowledge HERA being located in the rohe of Manukau, Tāmaki Makaurau (Auckland). The use of te reo Māori (the Māori language) is intentional as part of the programme's commitment to Vision Mātauranga. The authors also thank MM Group 3 Limited and WSP New Zealand for their cooperation and support in conducting structural health monitoring.

REFERENCES

Behmanesh, I., Moaveni, B., Lombaert, G., & Papadimitriou, C. (2015). Hierarchical Bayesian model updating for structural identification. *Mechanical systems and signal processing*, *64*, 360-376.

Ereiz, S., Duvnjak, I., & Jiménez-Alonso, J. F. (2022). Review of finite element model updating methods for structural applications. Structures,

Friswell, M. I., & Mottershead, J. (1995). *Finite element model updating in structural dynamics*. Kluwer Academic Publishers.

Kammer, D. C. (1991). Sensor placement for on-orbit modal identification and correlation of large space structures. *Journal of Guidance, Control, and Dynamics*, *14*(2), 251-259.

Konno, K., & Ohmachi, T. (1998). Ground-motion characteristics estimated from spectral ratio between horizontal and vertical components of microtremor. *Bulletin of the Seismological Society of America*, *88*(1), 228-241.

Moaveni, B., He, X., Conte, J. P., & Restrepo, J. I. (2010). Damage identification study of a seven-storey full-scale building slice tested on the UCSD-NEES shake table. *Structural Safety*, *32*(5), 347-356.

Monteiro, D. K. (2022). *Numerical implementation of the data-driven stochastic subspace identification (SSI-DATA)*. In Zenodo. https://doi.org/10.5281/zenodo.7352986

Peeters, B. (2000). System identification and damage detection in civil engineering.

Rocchetta, R., Broggi, M., Huchet, Q., & Patelli, E. (2018). On-line Bayesian model updating for structural health monitoring. *Mechanical systems and signal processing*, *103*, 174-195.

Sohn, H., Farrar, C. R., Hemez, F. M., Shunk, D. D., Stinemates, D. W., Nadler, B. R., & Czarnecki, J. J. (2003). A review of structural health monitoring literature: 1996–2001. *Los Alamos National Laboratory, USA*, *1*, 16.

Sohn, H., & Law, K. H. (1997). A Bayesian probabilistic approach for structure damage detection. *Earthquake engineering & structural dynamics*, *26*(12), 1259-1281.

Teughels, A., & De Roeck, G. (2004). Structural damage identification of the highway bridge Z24 by FE model updating. *Journal of Sound and Vibration*, *278*(3), 589-610.

Van Overschee, P., & De Moor, B. (2012). *Subspace identification for linear systems: Theory—Implementation—Applications*. Springer Science & Business Media.